Are Dawn Storms Jupiter's Auroral Substorms?

B. Bonfond[1] , Z. H. Yao[1,2] , G. R. Gladstone[3] , D. Grodent[1] , J.-C. Gérard[1] , J. Matar[1] , B. Palmaerts[1] , T. K. Greathouse[3] , V. Hue[3] , M. H. Versteeg[3] , J. A. Kammer[3] , R. S. Giles[3] , C. Tao[4] , M. F. Vogt[5] , A. Mura[6] , A. Adriani[6] , B. H. Mauk[7] , W. S. Kurth[8] , and S. J. Bolton[3]

[1]Laboratory for Planetary and Atmospheric Physics, Space Science, Technologies and Astrophysical Research Institute, University of Liège, Liège, Belgium, [2]Key Laboratory of Earth and Planetary Physics, Institute of Geology and Geophysics, Chinese Academy of Sciences, Beijing, China, [3]Southwest Research Institute, San Antonio, TX, USA, [4]National Institute of Information and Communications Technology, Tokyo, Japan, [5]Center for Space Physics, Boston University, Boston, MA, USA, [6]Institute for Space Astrophysics and Planetology, National Institute for Astrophysics, Rome, Italy, [7]Applied Physics Laboratory, Johns Hopkins University, Laurel, MD, USA, [8]Department of Physics and Astronomy, University of Iowa, Iowa City, IA, USA

Abstract Dawn storms are among the brightest events in the Jovian aurorae. Up to now, they had only been observed from Earth-based observatories, only showing the Sun-facing side of the planet. Here, we show for the first time global views of the phenomenon, from its initiation to its end and from the nightside of the aurora onto the dayside. Based on Juno's first 20 orbits, some patterns now emerge. Small short-lived spots are often seen a couple of hours before the main emission starts to brighten and evolve from a straight arc to a more irregular one in the midnight sector. As the whole feature rotates dawn-ward, the arc then separates into two arcs with a central initially void region that is progressively filled with emissions. A gap in longitude then often forms before the whole feature dims. Finally, it transforms into an equatorward-moving patch of auroral emissions associated with plasma injection signatures. Some dawn storms remain weak and never fully develop. We also found cases of successive dawn storms within a few hours. Dawn storms thus share many fundamental features with the auroral signatures of the substorms at Earth, despite the substantial differences between the dynamics of the magnetosphere at the two planets.

Plain Language Summary Polar aurorae are a direct consequence of the dynamics of the plasma in the magnetosphere. The sources of mass and energy differ between the Earth's and Jupiter's magnetospheres, leading to fundamentally distinct auroral morphologies and very different responses to solar wind variations. Here, we report on the imaging of all development stages of spectacular auroral events at Jupiter, called dawn storms, including, for the first time, their initiation on the nightside. Our results reveal surprising similarities with auroral substorms at Earth, which are auroral events stemming from explosive magnetospheric reconfigurations. These findings demonstrate that, whatever their sources, mass and energy do not always circulate smoothly in planetary magnetospheres. Instead they often accumulate until the magnetospheres reconfigure and generate substorm-like responses in the planetary aurorae, although the temporal and spatial scales are different for different planets.

1. Introduction

The specificity of the dawn storms among the various auroral morphologies at Jupiter was recognized as soon as the first high resolution ultraviolet (UV) images of the aurorae on Jupiter became available (Gérard et al., 1994). As observed from the Hubble Space Telescope (HST), having only access to the Earth-facing side of the aurora, they consist of a thickening and a major enhancement of the brightness of the dawn arc of the main auroral emission (main oval). They seem to last for at least 1–2 h (Ballester et al., 1996), but given the typical length of HST sequences is ∼45 min, HST could not provide a complete and uninterrupted view of the process. Dawn storms are also characterized by clear signatures of methane absorption, indicating that the charged particles causing them can precipitate deep below the methane homopause, with energies up to 460 keV (Gustin et al., 2006) in the case of electrons. Based on the large HST observation campaign carried out in 2007, dawn storms appeared rare (3 cases out of 54 observations) and occurred independently from the state of the solar wind (Nichols et al., 2009). However, the dawn storm observed

during the HST campaign supporting the Juno mission as it approached Jupiter in 2016 occurred just as a coronal mass ejection hit Jupiter's magnetosphere, re-igniting the debate on the relationship between dawn storms and solar wind fluctuations (Kimura et al., 2017).

Simultaneous in situ measurements in the dawn-side magnetosphere with Juno and auroral images from the HST showed that dawn storms are associated with reconnection, dipolarization and particle acceleration signatures (Z. H. Yao et al., 2020a, Swithenbank-Harris et al. 2021). Observations from Galileo also showed signatures of dipolarization, plasmoid release, and plasma energization in the magnetotail, which were associated with substorm-like events (Ge et al., 2007; Kronberg et al., 2005, 2008; Krupp et al., 1998), because of the analogy with similar processes taking place during terrestrial substorms. Magnetospheric substorms are defined as "a transient process initiated on the night side of the Earth in which a significant amount of energy derived from the solar wind-magnetosphere interaction is deposited in the auroral ionosphere and magnetosphere" (Rostoker et al., 1980). It is however unlikely that the solar wind, and especially dayside magnetopause reconnection, would play a similar role in the internally driven Jovian magnetosphere (Delamere & Bagenal, 2010).

So far, our understanding of auroral dawn storms has been incomplete mainly because we have been unable to observe the whole extent of the event, both temporally and spatially. New data from the Juno mission reveal for the first time where and how the dawn storms start and their consequences.

2. Image Processing

Juno is a NASA New Frontiers spacecraft orbiting Jupiter since July 4, 2016. Its 53-day eccentric polar orbit brings its perijove (PJ) to ~4,000 km above the surface (1 bar level) at low latitudes. This orbit allows its ultraviolet spectrograph (UVS) to acquire spectrally resolved images of the polar aurorae from ~4 h before the PJ (in the northern hemisphere) to ~4 h after PJ (in the southern hemisphere) with a ~1-h interruption in between during the closest approach at low latitude.

Juno-UVS is an imaging spectrograph operating in the 68–210 nm range (Gladstone et al., 2017; Greathouse et al., 2013). Its dog-bone shaped slit is 7.2° long, 0.025° wide in the center, and 0.2° wide in the two extremities. The slit is generally oriented perpendicularly to the Juno spin plane. However, a scan mirror located at the entrance of the instrument allows to shift the field of view by up to ±30° from the spin plane. In the present work, only the data from the wide parts of the slit are used, in order to optimize the signal-to-noise ratio. Moreover, the wavelength range from 155 to 162 nm is selected in order to avoid regions affected by absorption of the UV light by hydrocarbon molecules in the Jovian atmosphere (mostly methane) below 155 nm and by reflected sunlight beyond 162 nm.

The calibrated data from Juno-UVS are available through the Planetary Data System in the form of FITS files, which contain information about each event collected by the detector, such as the time of the event, its position in X and Y on the detector, the corresponding wavelength, etc. This first step of the processing consists of removing the noise due to particle (typically relativistic electrons) penetrating into the instrument and impacting the detector from the signal caused by UV photons. Contrary to photons, which are diffracted by the grating, penetrating particles illuminate the detector in an almost homogenous fashion, as confirmed by observations carried out in the radiation belts. We use a region between pixels 345–550 in the X direction (corresponding to ~59.7–80.9 nm) and pixels 20–255 in the Y direction, which has a very low effective area for extreme-UV photons (Hue et al., 2019), in order to estimate the count rate per pixel due to radiation. This background noise is then removed from the photon illuminated part of the detector.

The second step consists, for each detection event, of projecting the four corners of each field of view element along the slit onto a Jupiter-shaped ellipsoid located 400 km above the 1-bar level, using the SPICE kernels listed in the FITS file header. The brightness, derived from the weighted counts and the exposure time, is then attributed to a quadrilateral formed by these four points. A map of the aurora is then progressively built by adding all the detected events for a given Juno spin. Simultaneously, an exposure map, identifying the regions of the planet covered by the instrument's field of view, is also constructed. Images of the whole aurorae are then assembled by performing a weighted sum of the consecutive spins, with a higher weight being attributed to the latest spin. Going back in time, each weighting coefficient is 1/10th of

Table 1
List of the Dawn Storms Identified During Juno's Perijove Observations Sequences

	Date	Peak power (W)	Identified features
PJ1	27 Aug 2016 18:00 => **20:00**		b?, e
PJ3	11 Dec 2016 15:10 =>**22:02**	8.1 10¹¹	b, e, g, nids
PJ5	27 Mar 2017 **3:56** => 06:00	1.5 10¹¹	e, g, i, nids
	7:33=> 11:09	1.1 10¹¹	
PJ6	19 May 2017 07:14 => **10:54**	1.6 10¹²	b?, e, i
PJ7	10 Jul 2017 22:43 => 00:00	2.7 10¹¹	e, i
PJ9	24 Oct 2017 12:19 => 13:50	6.0 10¹¹	e
PJ11	07 Feb 2018 12:58 => **18:49**	8.5 10¹¹	s, b, e, g
PJ14	16 Jul 2018 08:42=> **10:15**	6.5 10¹¹	e
PJ16	29 Oct 2018 23:20=> 01:00	1.4 10¹¹	s, e, i?
PJ20	29 May 2019 09:30 => **12:54**	9.2 10¹¹	e, g, i

Note. The second column collects the approximate times of the expansion phases of the dawn storm. The end time, in particular, are approximate, as there is no clear criterion for when the phenomenon is finished. Start and end times in bold indicate that the observations started or ended at the indicated time, but the dawn storm probably lasted longer. The third column indicates the peak power reached by the dawn storm and the fourth column indicates the observed feature during this sequence, (s) meaning the spots, (b) the beads, (e) the expansion, (g) the gap, (i) the injections, and (nids) the occurrence of nonisolated dawn storms. The PJ1 dawn storm started after the end of the UVS observations, but the beginning of the expansion phase was observed with the JIRAM (Jovian InfraRed Auroral Mapper) instrument (Adriani et al., 2017; Mura et al., 2017) (Figure S9).

the previous one. We then divide the weighted sum of the counts with a weighted sum of the exposure maps to derive our final brightness map. This method offers the best compromise between the completeness of the auroral map and the dynamics of the auroral features. However, since UVS cannot observe the whole aurora during a given spin during the perijove sequence, the exact timing and duration of some transient events is uncertain, with temporal knowledge gaps of 30 s at best due to the spinning spacecraft.

Three main sources of uncertainty affect estimates of the total emitted power by the H_2 molecules in the UV: 1) systematic calibration uncertainties estimated on the order of 16% (Gérard et al., 2020), 2) shot noise uncertainty, which depends on the number of counts in the region of interest and is typically below 5% for the small spots and below 1% for the larger dawn storm features, and 3) the selection uncertainty, which depends on the way the region of interest is defined and which may reach up to 15%. The quadratic sum of all these uncertainties can be rounded to a reasonable value of 25% for power estimates.

3. Observations of Dawn Storms

3.1. Development Sequence of Typical Dawn Storms

For the first time, Juno-UVS granted us a complete and global picture of the auroral dawn storms, from their initiation to their vanishing. Indeed, Juno captured views of dawn storms at different stages of development in approximately half of the first 20 perijoves (Table 1).

For example, on February 7, 2018 (PJ11), Juno-UVS captured the initiation of a dawn storm from low altitude (~43,000 km) above the north pole, thus allowing unprecedented high spatial resolution observations (Figure 1). Around 13:06 UT, the event started with a relatively bright midnight arc (~2,000 kR). Then a few spots began to appear poleward of this arc, creating a string of approximately a dozen spots within 14 min, each one forming ~1,000 km duskward of the previous (Figure 2). These spots are ~1,000 km long (in the north-south direction) and ~150 km wide, which corresponds to the projection of the instrumental point spread function (PSF) on the planet. Hence, the apparent North-South extension probably result from the asymmetry of the PSF. They each typically emit ~1 GW of total power and appear with a peak brightness of ~800 kR. Using the flux mapping method of Vogt et al. (2015), but with JRM09 (Connerney et al., 2018) as an internal field model, these spots map to a distance of 65–110 Jovian radii (R_J) and a local time range between 22:40 UT and 23:45 UT, which broadly corresponds to the X-line, where magnetotail reconnections take place (Vogt et al., 2010). When mapped in the magnetosphere, the interspot distance corresponds to 1–2° of longitude, or to a mapped distance of 6–7 R_J. The distance between the mapped locations of the first (and dawn-most) and last (and dusk-most) spots is about 42 R_J (~3.10⁶ km), and the associated propagation speed would be on the order of 3,600 km/s in the azimuthal direction. If we focus on the brightest central spots, this apparent mapped azimuthal velocity reaches 10,000 km/s. If these spots indeed correspond to magnetic reconnection on the X-line, it is however quite likely that these high values do not correspond to any physical velocity in the magnetosheet, and that the time interval rather corresponds to a phase delay. Furthermore, these numbers should be considered as rough estimates only, since 1) the mapping uncertainty strongly increases with radial distance and 2) any static mapping model is inaccurate, whatever the planet, during magnetospheric reconfiguration events. Even though the spin modulated sampling rate of UVS does not allow for easy monitoring, individual spots appear to vanish after a few minutes. These short-lived spots may be similar to the midnight spots occasionally observed from the HST at the limb of the planet (Grodent et al., 2004; Radioti et al., 2011). Another example of transient bright spots was found during PJ16 (see Figure S1 in the supporting information).
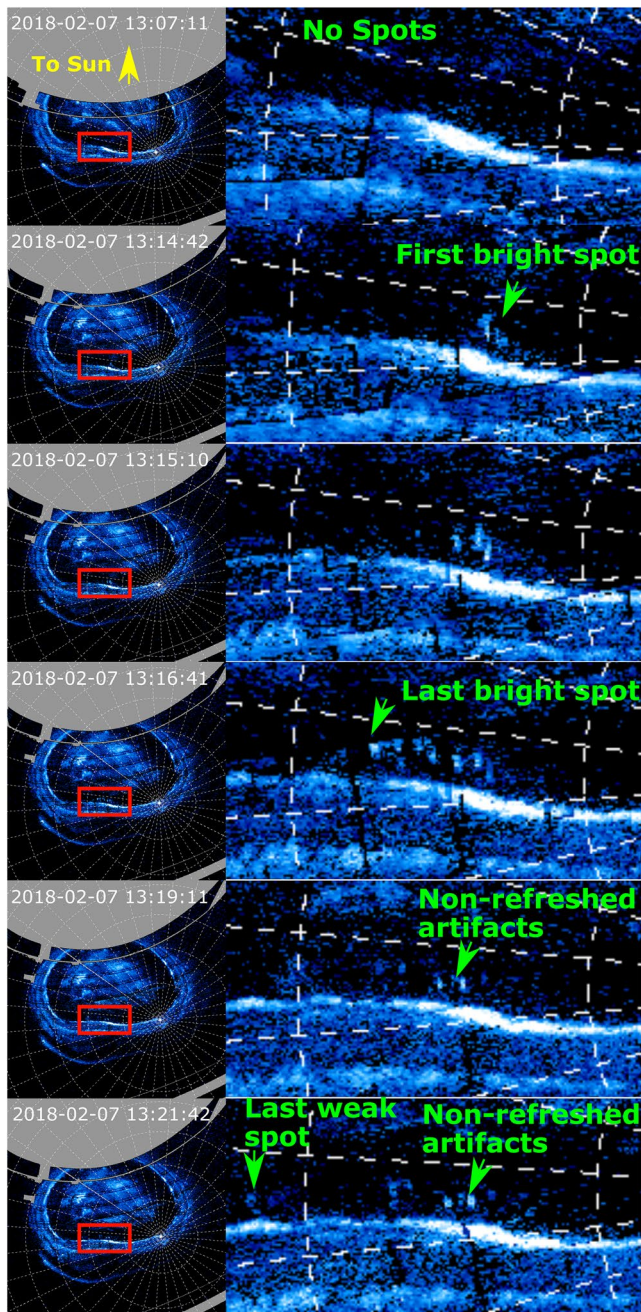
Figure 1. Details of the development of the transient spots during the PJ11 dawn storm. A polar projection of the whole northern aurora is shown on the left and a zoom on the region boxed in red is shown on the right. The Sun direction is toward the top and dashed lines show System III meridians and planeto-centric parallel spaced every 10°. Bright spots of the size of the instrumental PSF successively appeared from dawn to dusk, ~1,000 km apart. The two bright spots remaining on the center of the last two frames are due to the nonrefreshment of this part of the image.

Two hours later, Juno was located over the southern hemisphere when the main emission began to brighten and broaden irregularly, forming a bead-like pattern in the same midnight sector (Figure S2). Fly-bys carried out at lower altitude during this phase of the dawn storm, such as during PJ3 at 15:37 UT, render this pattern, with beads with ~1,500 km (~2°) spacing, even more obvious. Once mapped into the magnetodisk, these beads appear to originate from a region ~50 R_J from Jupiter and are azimuthally separated by ~8 R_J (3° of longitude) in the magnetospheric local time range between ~1:45 and ~3:00 LT. Hence, the enhancement of the main emission, leading to the full-fledged dawn storm, actually started around magnetospheric midnight. This feature then slowly migrated to the dawn sector at a pace corresponding to ~25% of corotation with the planet. Around 16:22 UT, the main arc split into two parts, with one moving ~2,500 km toward the pole while the other remain relatively still. Because it is likely that these auroral features arise from a reconfiguration of the magnetic field, static magnetic field mapping models would most probably provide misleading results. The whole feature continued to rotate, progressively accelerating toward corotation with the magnetic field as the dawn storm developed. Around 17:15 UT, the feature appeared to split, but longitudinally this time. The gap extends overs ~10° of longitude in the upper atmosphere. At its peak, the total power reached 850 GW, which is among the brightest events observed during Juno's first 20 orbits (see Table 1). The UVS perijove observations ended at 18:50 UT, even though the event was still ongoing.

On May 19, 2017 (PJ6), the Juno-UVS observations missed the beginning of an event, but allowed us to examine the next phases. After the broadening and the latitudinal splitting of the main emission, the outer-most arc transformed into large patches. On the same day, subsequent HST images acquired with the Space Telescope Imaging Spectrograph (STIS) confirmed that the patches continued their evolution, forming latitudinally extended fingers slowly expanding equatorward. Such features have been associated with large and fresh plasma injection signatures (Dumont et al., 2018). While such a connection between dawn storms and large injection signatures has been proposed previously, based on the simultaneous presence of a dawn storm and large injection signatures on the same image (Gray et al., 2016; Grodent et al., 2018), this long and continuous set of observations from Juno and Hubble is the first to clearly demonstrate the transition from one into the other. It should also be noted that some (less intense) injection signatures can also appear independently from dawn storms, as was observed during PJ1 for example (Bonfond et al., 2017).

3.2. Nonisolated Dawn Storms

Juno-UVS observations of dawn storms show that they sometimes occur as a series, rather than isolated events. For example, on March 27, 2017 (PJ5), a first dawn storm was ongoing when the observations started at 03:57 UT and was finished by ~06:51 UT, after which a second one was observed peaking around 08:08 UT. Figure 3 (top) show the aurora at 04:06, during the first brightening, at 07:25, after it finished and at 08:08, during the second brightening. In other cases, there appears to be no gap between consecutive events. For example, during PJ3 (December 11, 2016), the dawn storm expansion phase seemed to never really stop, continuously going on at the same local time. The dawn storm was first observed with the apparition of beads around 15:21 UT, as Juno was flying over the northern hemisphere, and continued until auroral
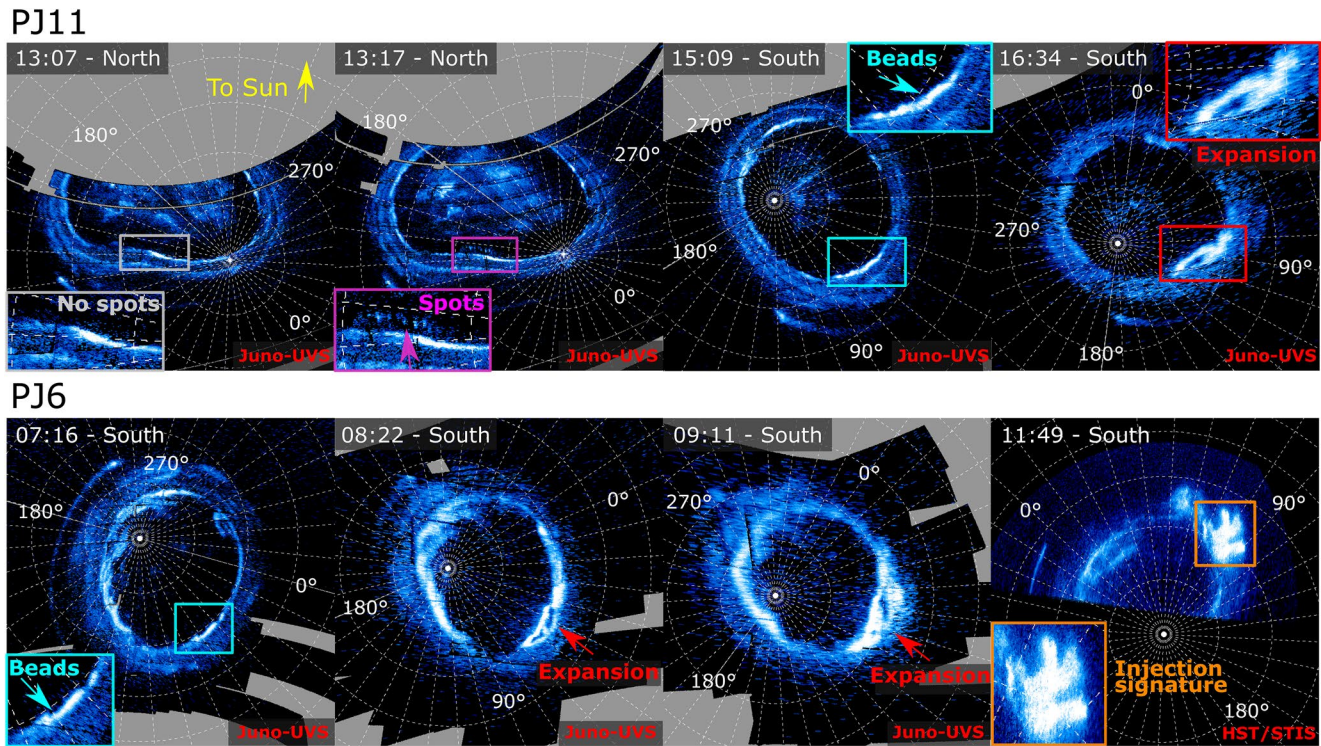
Figure 2. Polar projection of the development of a dawn storm, based on observations acquired by Juno-UVS and HST/STIS during the 11th and the 6th perijove sequences. On PJ11, the event was preceded by the progressive appearance of a set of transient spots poleward of the main emission. Two hours later, the dawn storm itself started as an enhancement of the main emission in the form of beads before the arc began to fork and expand, both latitudinally and longitudinally. On the PJ6 sequence, the same sequence of emergence of beads, followed by the expansion phase is observed, but subsequent observations by both Juno-UVS and HST-STIS show that the equatorward arc transforms into a large injection signature.

observations were interrupted by Juno's low latitude fly-by. When observations of the southern hemisphere started over, a dawn storm was still ongoing and this continued until the end of the sequence at 22:01 UT, with the emitted power increasing around the end.

3.3. Pseudo-dawn storms

During PJ16 (October 29, 2018), Juno-UVS observed the development of a particularly limited dawn storm-like event (Figure 4). Around 20:19 UT, the instrument captured the appearance of three transient (~6 min) spots poleward of the midnight arc of the main emission. Moreover, the midnight arc itself was fainter than during PJ11 and the number of spots was also smaller. The brightness of the enhanced the dawn arc of the main emission observed at 23:39 UT was fairly dim (~500 kR), and the area concerned with the enhancement was limited (~10° in longitude). While the sequence of events is similar to the one observed on PJ11, which is why we identify it here as a dawn storm, it would probably not have qualified as a dawn storm in previous studies, due to its limited extent and brightness. This reason, together with the fact that Juno observes the whole auroral region, including the nightside where dawn storms arise, almost continuously for ~8 h explains the discrepancy between our detection rate and the one deduced from HST, which only focused on the dawn storm expansion phase. The second dawn storm on PJ5 is another example of such a limited dawn storm (Figure 3, top right panel).

4. Discussion

Put together, the Juno-UVS observations paint a brand new picture of dawn storms. They consist of a 5–10 h long chain of events, starting with the transient spots (Figure S1), followed 2–3 h hours later by the formation of bead-like features on the midnight part of the main emissions (Figure S2). This time delay between
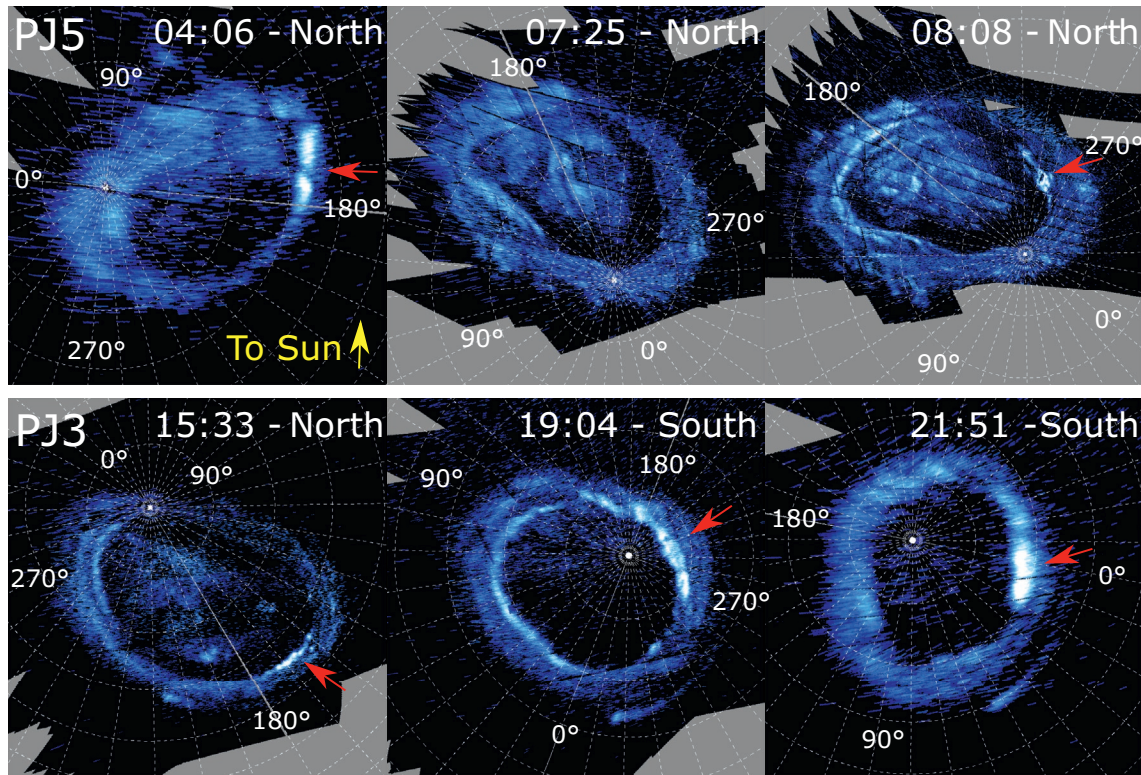
Non-Isolated Dawn Storms

Figure 3. Polar projections of the development of nonisolated dawn storms during PJ3 and PJ5. The red arrow highlights the dawn storms. During PJ5, a second dawn storm took place ~3 h after the first one. On PJ3, new dawn storms seem to appear during all the southern branch of the perijove sequence.

events taking place at 90 and 50 R_J, respectively, suggests a propagation speed of 250–400 km/s, which is consistent with estimates of the fast mode velocity in the plasma sheet (Kivelson, 2015; Manners et al., 2018). This is followed by a longitudinal and latitudinal (mostly poleward) expansion phase, during which the main emission brightens, expands, thickens, and forks into two branches (Figure S3 in the supporting information). This chain of events is very similar to the one observed during terrestrial auroral substorms (Figure 5). Substorms are global reconfigurations of the magnetosphere during which the magnetic energy stored in the magnetotail is converted into particle energy, which lead to spectacular auroral brightening in nightside polar regions which generally follow a well-established sequence of features (Akasofu, 2013). The transient spots observed in Jupiter's aurora share several morphological and temporal characteristics with transient mesoscale features on Earth, sometimes associated with poleward boundary intensifications and sometimes with streamers (Forsyth et al., 2020). Both are often observed before the substorm onset (Nishimura et al., 2011), even if the exact relationship between streamers and substorms is disputed (Miyashita & Ieda, 2018). Both phenomena are associated with reconnection in the magnetotail and the subsequent inward flow of plasma and dipolarizing field lines (Angelopoulos et al., 2008). At Jupiter, the tentative connection between magnetotail reconnection and dawn storm has been evocated by several authors (Ballester et al., 1996; Ge et al., 2010). Recently, the most compelling examples of such a connection come from contemporaneous in situ particle and fields measurements by Juno and HST images of the aurora (Z. H. Yao et al., 2020a). These observations show large reconnection signatures on magnetic field lines mapping poleward of a dawn storm and then dipolarization signatures preceding auroral injection signatures. The preexpansion beads observed in the context of terrestrial substorms (Henderson, 2009) are associated with plasma instabilities in the near magnetotail, such as the ballooning instability (Z. Yao et al., 2017). The expansion phases of Jupiter's dawn storms and the Earth's substorms also share fundamental similarities, and the latter is known to be associated with a dipolarization/current disruption in the magnetosphere. In particular, the apparition of a bifurcated oval at Jupiter resembles terrestrial bulge-type aurora observed during
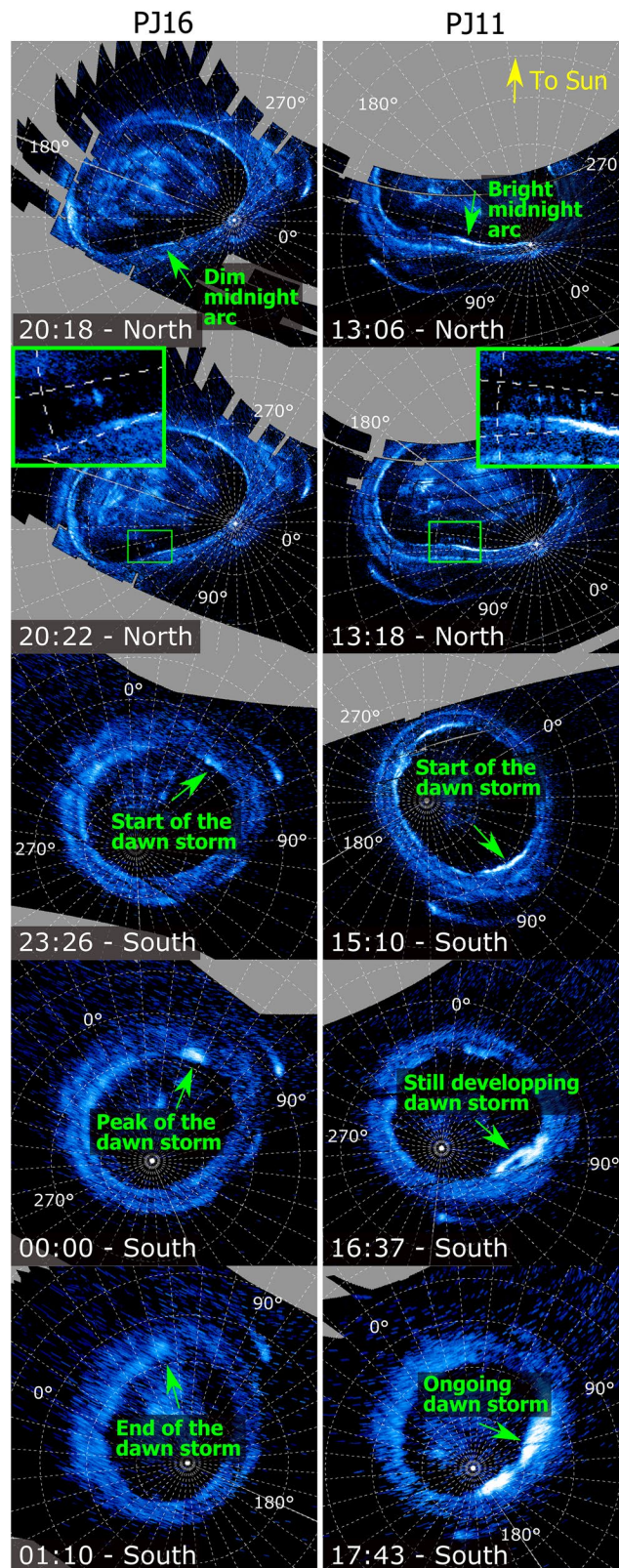
Figure 4. The left column shows polar projections of the aurorae during the 16th perijove, and the right column shows a similar sequence for the 11th perijove. While the sequence on PJ11 compares with a terrestrial substorm (Figure 1), the one on PJ16 is much more limited in size, emitted power and duration and would be more similar to a terrestrial pseudo-breakup.
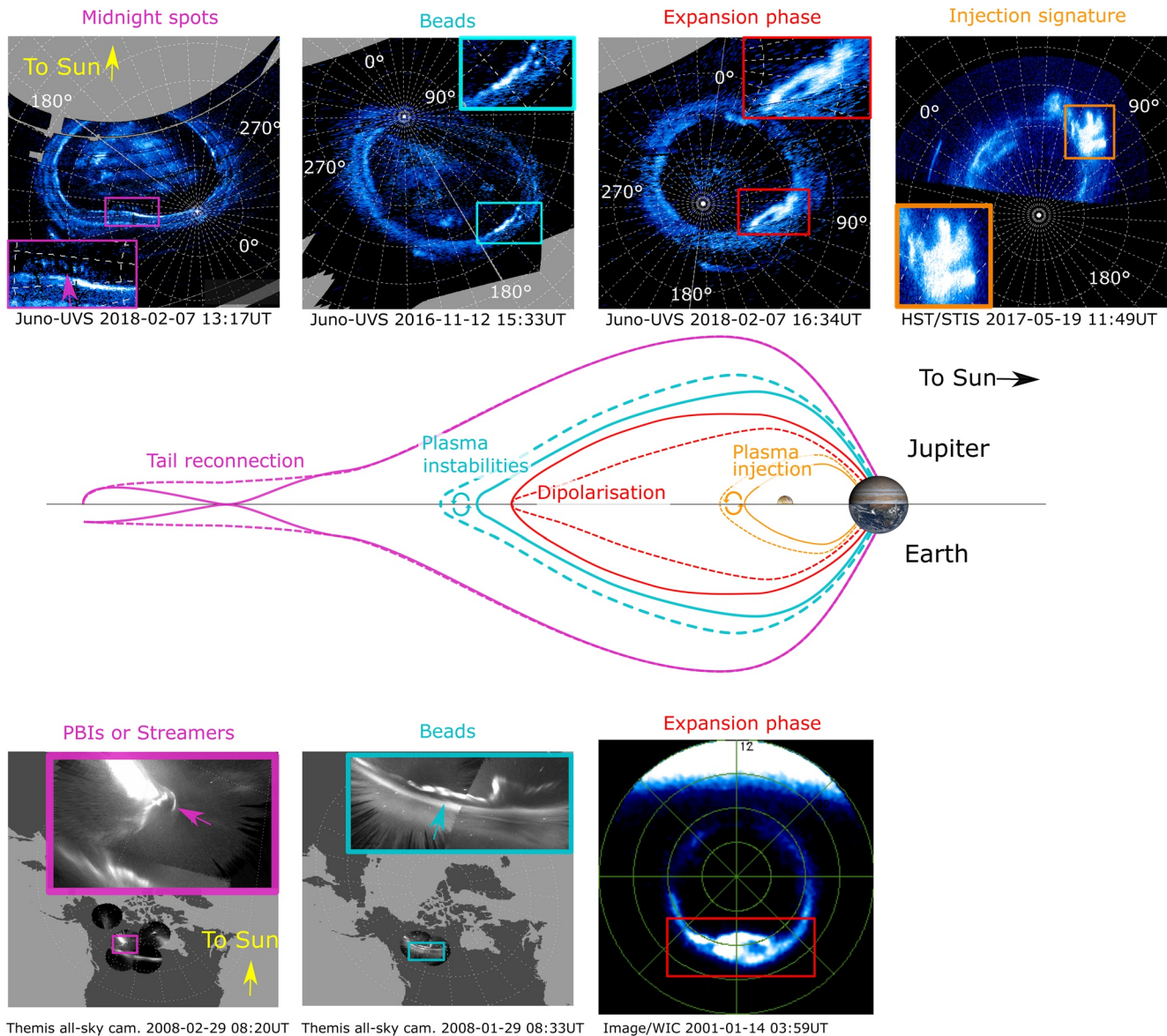
Figure 5. Polar projections of the UV aurora showing four different phases of a Jovian dawn storm: 1) the short lived polar midnight spots, 2) the formation of irregularities on the main emission predawn part 3) the expansion phase, with the two arcs splitting, and 4) the injection signatures in the outer emission. The first three images are based on data from the Juno-UVS instrument and the fourth one comes from Hubble Space Telescope observations carried out to support Juno. These four phases appear to correspond to nightside tail reconnection, plasma instabilities, current disruption/dipolarization in the middle magnetosphere and to flux tube interchange, respectively, as illustrated in the general scheme shown in the central scheme (not to scale). These auroral features corresponding to these phases in the terrestrial aurora are show on the bottom raw. In the bottom, the first two images come from the THEMIS network of all-sky cameras (Nishimura et al., 2010; Z. Yao et al., 2017). The third image corresponds to Earth's aurora as seen from IMAGE-WIC.

substorms (Gjerloev et al., 2007, 2008). Finally, the auroral patches in the equatorward emissions manifest massive plasma injections (Figure S6). Plasma injections in the inner terrestrial magnetosphere are indeed observed by in situ instruments during substorm events (Gabrielse et al., 2019) and they can also give rise to equatorward moving auroral enhancements (Sergeev et al., 2010). One notable difference is that auroral substorms do not rotate with the Earth, but evolve in fixed local time, that is, around midnight (with a slight preference at premidnight [Gjerloev et al., 2004]).

At Earth, substorms do not always occur as isolated events. Instead, multiple substorm expansions can happen consecutively (Liou et al., 2013). A similar behavior is observed for dawn storms at Jupiter. The occurrence of successive dawn storms separated by a delay of a few hours could explain why images of dawn

storms from HST often display large injection signatures in the postnoon sector (Gray et al., 2016; Grodent et al., 2018). Furthermore, Z. H. Yao et al. (2020a) suggest that successive dawn storms are responsible for the multiple injection auroral structures.

Terrestrial substorms vary considerably in intensity and those which could not fully develop are called pseudo-breakups (Pulkkinen et al., 1998). The event observed during PJ16 (October 29, 2018) was limited to a small intensification, which might be analogous to terrestrial pseudo-breakups (Figure 4).

The orientation of the interplanetary magnetic field (and, to a lesser extent, the dynamic pressure of the solar wind) controls the occurrence and intensity of Earth substorms (Kullen & Karlsson, 2004). Unfortunately, these solar wind parameters are difficult to obtain at Jupiter while Juno carries out its perijove observations. Therefore, we used the propagation model from Tao et al. (2005), which relies on measurements acquired at one astronomical unit from the Sun (from either the OMNI data or the Stereo A spacecraft) to estimate the solar wind velocity and dynamic pressure at Jupiter when Jupiter and the observatory are sufficiently well aligned (<40°) (Figures S6–S8). Most dawn storms for which such an estimate was possible (i.e., PJ5, PJ9, PJ14, and PJ20) happened more than 2 days away from any solar wind enhancement, which confirms that dawn storm may occur during relaxed solar wind conditions. However, they can also occur at times closer to a solar wind enhancement (e.g., PJ1, PJ6, and PJ16), suggesting that solar wind shocks do not necessarily prevent their occurrence. The comparison of the location of the magnetopause measured by Juno and the aurora observed by HST also suggests that dawn storms happen independently of the state of compression of the magnetosphere and are most probably internally driven, contrary to the global main emission brightenings, which only occur in the compressed state (Z. H. Yao et al., 2020b).

Despite the similarities between terrestrial substorms and Jovian dawn storms, it is also important to stress the major differences between the Earth's and Jupiter's magnetospheres (B. Mauk & Bagenal, 2013). The first is dominated by its interaction with the solar wind, and magnetic reconnections on the dayside magnetopause drive the plasma convection in the magnetosphere through the so-called Dungey cycle (Dungey, 1961). On the other hand, the Jovian magnetosphere is inflated with plasma originating from the volcanic moon Io and the rotation of the planet controls the motion and the energization of the magnetospheric plasma. The mechanism through which the mass injected at Io is ultimately released via reconnection on closed field lines is called the Vasyliunas cycle (Kronberg et al., 2007; Vasyliunas, 1983). Reconnection on the dayside magnetopause, while it does exist at Jupiter (Ebert et al., 2017), cannot open a significant amount of flux (Desroche et al., 2012; Masters, 2017), leading to a very different type of magnetospheric topology where the amount of flux open to the solar wind is very limited and intertwined with closed flux tubes connected to the distant magnetotail (Zhang et al., 2020). By comparing the occurrence of magnetotail reconnection and plasmoid release to predictions of the solar wind input (Vogt et al., 2019), showed that these large scale reconfigurations of the magnetotail were mostly independent from solar wind compression.

However, regardless of the different reasons for the loading, in both cases plasma and energy regularly accumulate within the system, which grows increasingly unstable, especially in the midnight magnetotail where the field lines are the most elongated. While the long term (∼months) global evolution of the position of the main auroral emissions has been attributed to the variations of the mass output from Io (Bonfond et al., 2012), the shorter term variations of its position at different local times are poorly understood. Hence, since its typical location at midnight for the various System III longitudes is unknown, we were unable to identify any equatorward departure from it, as typically observed for the terrestrial growth phase auroral arcs.

The stretching of the field lines provides favorable conditions for reconnection to occur. At Earth, such reconnection closes the magnetic field lines open to the solar wind in the magnetotail, while at Jupiter, reconnection is internally driven (Ge et al., 2010; Kronberg et al., 2005; Vogt et al., 2019; Woch et al., 2002) and is expected to take place on closed field lines. In the middle magnetosphere, various plasma instabilities may occur, such as ballooning instability (Hameiri et al., 1991; Kalmoni et al., 2018; Oberhagemann & Mann, 2020), cross-field current instability (Lui et al., 1991), shear flow ballooning (Viñas & Madden, 1986) or shear flow-interchange instability (Derr et al., 2020). Since the magnetic field lines in Jupiter's outer magnetosphere are also highly stretched, and the magnetosphere consists of more energetic ions than the Earth's magnetotail, many plasma instabilities identified in Earth's magnetotail would likely take place in

Jupiter's outer magnetosphere. Such instabilities can then lead to a disruption of the azimuthal currents in the middle magnetosphere and a dipolarization of the field lines. While the dipolarizing field lines would remain in the night sector at Earth, they would be progressively swept away in azimuthal direction by the planetary rotation at Jupiter as they progress inward. This makes studies of east-ward or west-ward expansion of the dawn storm almost impossible at Jupiter, because the exact longitudinal expansion would be very difficult to disentangle from partial corotation. These processes would also bring hot and sparse plasma from the outer magnetosphere further into the system and energize it, forming plasma injections (Z. H. Yao et al., 2020a). Their study also shows that dipolarization at Jupiter may corotate with the planet, as a counterpart of corotating auroral injection.

The above explanation probably gives the impression that the dawn storm auroral sequence implies that the magnetotail reconfigurations at Jupiter are systematically "outside-in" in nature, rather than "inside-out,". Here the "outside-in" means starting with reconnection at ∼90 R_J before propagating inward and disrupt the plasma sheet closer to Jupiter (∼60-40 R_J, where the main emissions map) and finally trigger plasma injections in the middle magnetosphere (30-10 R_J) and "inside-out" means starting in the middle magnetosphere with plasma injections, before disrupting the region where the main emissions maps (40–60 R_J) and finally triggering reconnection and the release of plasmoids in the distant magnetotail (∼90 R_J). For the terrestrial case, this debate around models such as the near-Earth neutral line model (outside-in) (Baker et al., 1996) and near Earth current disruption model (inside-out) (Lui, 2015) has been raging for years despite the flotilla of dedicated spacecraft cruising in the magnetosphere and we certainly would not want to suggest that with the few cases presented here, Juno has single handedly solved the problem at Jupiter. As a possible counter-example, the auroral observations during PJ1 with Juno-UVS have shown the progressive development of injection signature all around the pole before a poleward protrusion (the shape of which may be reminiscent of omega bands at Earth) appeared on the midnight arcs of the main emissions (Bonfond et al., 2017). It then took 2 h for bead-like features and then a dawn storm expansion phase to appear on infrared images (see Figure S9). Contrary to the other sequences discussed here, this particular one thus suggests that magnetospheric instabilities appeared closer to Jupiter before they developed further out. Some studies also suggested that both situations might appear at Earth (Murphy et al., 2014; Panov et al., 2020). Rather than a unique causal process leading to systematic chain of events, a possible interpretation is that the accumulation of mass and energy makes the different regions of the magnetosphere progressively susceptible to different types of plasma instabilities (including, at places, reconnection). Once one of these regions reaches the instability threshold and collapses, the generated disturbance propagates to the other regions, making their own collapse more likely.

While they have some unique characteristics as well, the magnetosphere and aurorae at Saturn are generally understood as representing an intermediate case between the Earth and Jupiter. Indeed several lines of evidence (Bader et al., 2019) show that Saturn supports a combination of Vasyliunas and rotating Dungey cycles (Cowley et al., 2005). It is thus less of a surprise to find similar auroral features, such as transpolar arcs (Radioti et al., 2013) or auroral beads (Radioti et al., 2019) in both the terrestrial and the Kronian aurorae. On the other hand, both observational and theoretical arguments indicate that the overall dynamics of the plasma in the terrestrial and jovian magnetospheres are fundamentally different (Delamere & Bagenal, 2010; Delamere et al., 2015; Louarn et al., 2000), one being mostly externally driven and the other being mostly internally driven. It is thus remarkable that universal processes releasing the accumulated matter and energy from the systems generate strikingly similar auroral signatures.

Finally, we note that, if our interpretation is correct, the evolution of the dawn storms is another demonstration that many, if not most, auroral processes and Jupiter cannot be explained by the corotation enforcement currents paradigm (Bonfond et al., 2020). Indeed, on both planets, currents and auroral intensities appear directly correlated only in specific places (Korth et al., 2014).

5. Summary and Conclusions

Freed from all the biases related to Earth-based observations, we detected dawn storms in approximately half of the Juno perijove sequences (10 dawn storm observations over 19 orbits—no observations were carried out during PJ2). This is due to three factors: 1) longer observations, providing additional chances

to catch dawn storm at any stage of their development, 2) a view of the nightside, where the dawn storms actually form, and 3) a looser definition of the dawn storm, which is no longer restricted to the brighter examples. Moreover, the occurrence of dawn storms appears independent of the arrival of a solar wind compression region at Jupiter.

While every feature has not been observed in each case, the dawn storms appear to follow a systematic sequence of events (Figure 5), some of which are being reported here for the first time. A dawn storm precursor appears to be the appearance of a series of transient spots separated by ∼1,000 km, mapping to the premidnight sector. Approximately 2–3 h later, the midnight section of the main emission starts to brighten, often forming regularly spaced (∼1,500 km apart) beads. The arc further brightens and expands in longitude as it progressively starts to corotate with the planet and to move toward the dawn side. Then it bifurcates, with a branch moving poleward. The void between the arcs then fills progressively as the arcs broaden in latitude. A longitudinal gap also generally forms within the feature. Finally, the whole feature dims and the equatorward part of the dawn storms evolves as an equatorward patch of emission associated with plasma injection signatures, providing a direct link between dawn storms and some plasma injection signatures.

Many of these auroral forms at Jupiter resemble mesoscale (Forsyth et al., 2020) and large-scale auroral forms observed during substorms at Earth. Furthermore, we found cases of consecutive dawn storms occurring within a few hours, similar to the nonisolated substorms at Earth. We also found cases of particularly weak dawn storm, reminiscent of pseudo-breakups at Earth.

The magnetospheric processes associated with substorm magnetotail reconfigurations, such as tail reconnection, dipolarization, or hot plasma injection have also been observed at Jupiter (Kronberg et al., 2005; Louarn et al., 2014; B. H. Mauk et al., 1997; Vogt et al., 2010; Woch et al., 2002). The connection between these processes and dawn storms, was proposed based on measurements from either in situ magnetic field or auroral images (Ge et al., 2010; Kimura et al., 2017), and was later confirmed by contemporaneous measurements from Juno and HST (Z. H. Yao et al., 2020a), associated with dawn storms. Despite the fact that the mass and energy loading in the magnetotail at Earth and Jupiter are very different, the evidence presented here show that the auroral signatures of the processes releasing them at Jupiter are remarkably similar to terrestrial auroral substorm.

Data Availability Statement

The data included herein are either archived in NASA's Planetary Data System (http://pds-atmospheres. nmsu.edu/data_and_services/atmospheres_data/JUNO/juno.html). This research is also based on publicly available observations acquired with the NASA/ESA Hubble Space Telescope and obtained at the Space Telescope Science Institute, which is operated by AURA for NASA (https://archive.stsci.edu/hst/search.php). Data analysis was performed with the AMDA science analysis system provided by the Centre de Données de la Physique des Plasmas (CDPP) supported by CNRS, CNES, Observatoire de Paris and Université Paul Sabatier, Toulouse. The THEMIS data are available from http://themis.ssl.berkeley.edu/data/themis/. The IMAGE-WIC images can be accessed at https://spdf.gsfc.nasa.gov/pub/data/image/fuv/and were processed using the FUVIEW3 software (http://sprg.ssl.berkeley.edu/image/).

References

Adriani, A., Filacchione, G., Di Iorio, T., Turrini, D., Noschese, R., Cicchetti, A., et al. (2017). JIRAM, the Jovian Infrared Auroral Mapper. *Space Science Reviews*, *213*(1), 393–446. https://doi.org/10.1007/s11214-014-0094-y

Akasofu, S.-I. (2013). Auroral morphology: A historical account and major auroral features during auroral substorms. In A. Keiling, E. Donovan, F. Bagenal, & T. Karlsson (Eds.), *Auroral phenomenology and magnetospheric processes: Earth and other planets* (pp. 29–38). American Geophysical Union (AGU). https://doi.org/10.1029/2011GM001156

Angelopoulos, V., McFadden, J. P., Larson, D., Carlson, C. W., Mende, S. B., Frey, H., et al. (2008). Tail reconnection triggering substorm onset. *Science*, *321*(5891), 931–935. https://doi.org/10.1126/science.1160495

Bader, A., Badman, S. V., Cowley, S. W. H., Yao, Z. H., Ray, L. C., Kinrade, J., et al. (2019). The dynamics of Saturn's main aurorae. *Geophysical Research Letters*, *46*(17–18), 10283–10294. https://doi.org/10.1029/2019GL084620

Baker, D. N., Pulkkinen, T. I., Angelopoulos, V., Baumjohann, W., & McPherron, R. L. (1996). Neutral line model of substorms: Past results and present view. *Journal of Geophysical Research*, *101*(A6), 12975–13010. https://doi.org/10.1029/95JA03753

Ballester, G. E., Clarke, J. T., Trauger, J. T., Harris, W. M., Stapelfeldt, K. R., Crisp, D., et al. (1996). Time-resolved observations of Jupiter's far-ultraviolet aurora. *Science*, *274*, 409–413. https://doi.org/10.1126/science.274.5286.409

Bonfond, B., Gladstone, G. R., Grodent, D., Greathouse, T. K., Versteeg, M. H., Hue, V., et al. (2017). Morphology of the UV aurorae Jupiter during Juno's first perijove observations. *Geophysical Research Letters*, *44*(10), 4463–4471. https://doi.org/10.1002/2017GL073114

Bonfond, B., Grodent, D., Gérard, J.-C., Stallard, T., Clarke, J. T., Yoneda, M., et al. (2012). Auroral evidence of Io's control over the magnetosphere of Jupiter. *Geophysical Research Letters*, *39*, L01105. https://doi.org/10.1029/2011GL050253

Bonfond, B., Yao, Z., & Grodent, D. (2020). Six pieces of evidence against the corotation enforcement theory to explain the main aurora at Jupiter. *Journal of Geophysical Research: Space Physics*, *125*(11), e2020JA028152. https://doi.org/10.1029/2020JA028152

Connerney, J. E. P., Kotsiaros, S., Oliversen, R. J., Espley, J. R., Joergensen, J. L., Joergensen, P. S., et al. (2018). A new model of Jupiter's magnetic field from Juno's first nine orbits. *Geophysical Research Letters*, *45*(6), 2590–2596. https://doi.org/10.1002/2018GL077312

Cowley, S. W. H., Badman, S. V., Bunce, E. J., Clarke, J. T., Gérard, J.-C., Grodent, D., et al. (2005). Reconnection in a rotation-dominated magnetosphere and its relation to Saturn's auroral dynamics. *Journal of Geophysical Research*, *110*, A02201. https://doi.org/10.1029/2004JA010796

Delamere, P. A., & Bagenal, F. (2010). Solar wind interaction with Jupiter's magnetosphere. *Journal of Geophysical Research*, *115*, A10201. https://doi.org/10.1029/2010JA015347

Delamere, P. A., Bagenal, F., Paranicas, C., Masters, A., Radioti, A., Bonfond, B., et al. (2015). Solar wind and internally driven dynamics: Influences on magnetodiscs and auroral responses. *Space Science Reviews*, *187*(1), 51–97. https://doi.org/10.1007/s11214-014-0075-1

Derr, J., Horton, W., & Wolf, R. (2020). Shear flow-interchange instability in nightside magnetotail as proposed cause of auroral beads as a signature of substorm onset. *Journal of Geophysical Research: Space Physics*, *125*(1), e2019JA026885. https://doi.org/10.1029/2019JA026885

Desroche, M., Bagenal, F., Delamere, P. A., & Erkaev, N. (2012). Conditions at the expanded Jovian magnetopause and implications for the solar wind interaction. *Journal of Geophysical Research*, *117*, A07202. https://doi.org/10.1029/2012JA017621

Dumont, M., Grodent, D., Radioti, A., Bonfond, B., Roussos, E., & Paranicas, C. (2018). Evolution of the auroral signatures of Jupiter's magnetospheric injections. *Journal of Geophysical Research: Space Physics*, *123*, 8489–8501. https://doi.org/10.1029/2018JA025708

Dungey, J. W. (1961). Interplanetary magnetic field and the auroral zones. *Physical Review Letters*, *6*(2), 47–48. https://doi.org/10.1103/PhysRevLett.6.47

Ebert, R. W., Allegrini, F., Bagenal, F., Bolton, S. J., Connerney, J. E. P., Clark, G., et al. (2017). Accelerated flows at Jupiter's magnetopause: Evidence for magnetic reconnection along the dawn flank. *Geophysical Research Letters*, *44*(10), 4401–4409. https://doi.org/10.1002/2016GL072187

Forsyth, C., Sergeev, V. A., Henderson, M. G., Nishimura, Y., & Gallardo-Lacourt, B. (2020). Physical processes of meso-scale, dynamic auroral forms. *Space Science Reviews*, *216*(4), 46. https://doi.org/10.1007/s11214-020-00665-y

Gabrielse, C., Spanswick, E., Artemyev, A., Nishimura, Y., Runov, A., Lyons, L., et al. (2019). Utilizing the heliophysics/geospace system observatory to understand particle injections: Their scale sizes and propagation directions. *Journal of Geophysical Research: Space Physics*, *124*(7), 5584–5609. https://doi.org/10.1029/2018JA025588

Ge, Y. S., Jian, L. K., & Russell, C. T. (2007). Growth phase of Jovian substorms. *Geophysical Research Letters*, *34*, L23106. https://doi.org/10.1029/2007GL031987

Ge, Y. S., Russell, C. T., & Khurana, K. K. (2010). Reconnection sites in Jupiter's magnetotail and relation to Jovian auroras. *Planetary and Space Science*, *58*(11), 1455–1469. https://doi.org/10.1016/j.pss.2010.06.013

Gérard, J.-C., Gkouvelis, L., Bonfond, B., Grodent, D., Gladstone, G. R., Hue, V., et al. (2020). Spatial distribution of the Pedersen conductance in the Jovian aurora from Juno-UVS spectral images. *Journal of Geophysical Research: Space Physics*, *125*, e2020JA028142. https://doi.org/10.1029/2020JA028142

Gérard, J. C., Grodent, D., Dols, V., Prangé, R., Waite, J. H., Gladstone, G. R., et al. (1994). A remarkable auroral event on Jupiter observed in the ultraviolet with the Hubble Space Telescope. *Science*, *266*(5191), 1675–1678. https://doi.org/10.1126/science.266.5191.1675

Gjerloev, J. W., Hoffman, R. A., Friel, M. M., Frank, L. A., & Sigwarth, J. B. (2004). Substorm behavior of the auroral electrojet indices. *Annales Geophysicae*, *22*(6), 2135–2149. https://doi.org/10.5194/angeo-22-2135-2004

Gjerloev, J. W., Hoffman, R. A., Sigwarth, J. B., & Frank, L. A. (2007). Statistical description of the bulge-type auroral substorm in the far ultraviolet. *Journal of Geophysical Research*, *112*, A07213. https://doi.org/10.1029/2006JA012189

Gjerloev, J. W., Hoffman, R. A., Sigwarth, J. B., Frank, L. A., & Baker, J. B. H. (2008). Typical auroral substorm: A bifurcated oval. *Journal of Geophysical Research*, *113*, A03211. https://doi.org/10.1029/2007JA012431

Gladstone, G. R., Persyn, S. C., Eterno, J. S., Walther, B. C., Slater, D. C., Davis, M. W., et al. (2017). The ultraviolet spectrograph on NASA's Juno Mission. *Space Science Reviews*, *213*(1), 447–473. https://doi.org/10.1007/s11214-014-0040-z

Gray, R. L., Badman, S. V., Bonfond, B., Kimura, T., Misawa, H., Nichols, J. D., et al. (2016). Auroral evidence of radial transport at Jupiter during January 2014. *Journal of Geophysical Research: Space Physics*, *121*(10), 9972–9984. https://doi.org/10.1002/2016JA023007

Greathouse, T. K., Gladstone, G. R., Davis, M. W., Slater, D. C., Versteeg, M. H., Persson, K. B., et al. (2013). Performance results from in-flight commissioning of the Juno Ultraviolet Spectrograph (Juno-UVS). In Proceedings of the SPIE (Vol. 8859, p. 2013). International Society for Optics and Photonics. https://doi.org/10.1117/12.2024537

Grodent, D., Bonfond, B., Yao, Z., Gérard, J.-C., Radioti, A., Dumont, M., et al. (2018). Jupiter's aurora observed with HST during Juno Orbits 3 to 7. *Journal of Geophysical Research: Space Physics*, *123*(5), 3299–3319. https://doi.org/10.1002/2017JA025046

Grodent, D., Gérard, J.-C., Clarke, J. T., Gladstone, G. R., & Waite, J. H. (2004). A possible auroral signature of a magnetotail reconnection process on Jupiter. *Journal of Geophysical Research*, *109*, A05201. https://doi.org/10.1029/2003JA010341

Gustin, J., Cowley, S. W. H., Gérard, J.-C., Gladstone, G. R., Grodent, D., & Clarke, J. T. (2006). Characteristics of Jovian morning bright FUV aurora from Hubble Space Telescope/Space Telescope Imaging Spectrograph imaging and spectral observations. *Journal of Geophysical Research*, *111*, A09220. https://doi.org/10.1029/2006JA011730

Hameiri, E., Laurence, P., & Mond, M. (1991). The ballooning instability in space plasmas. *Journal of Geophysical Research*, *96*(A2), 1513–1526. https://doi.org/10.1029/90JA02100

Henderson, M. G. (2009). Observational evidence for an inside-out substorm onset scenario. *Annales Geophysicae*, *27*(5), 2129–2140. https://doi.org/10.5194/angeo-27-2129-2009

Hue, V., Gladstone, G. R., Greathouse, T. K., Kammer, J. A., Davis, M. W., Bonfond, B., et al. (2019). In-flight characterization and calibration of the Juno-ultraviolet Spectrograph (Juno-UVS). *The Astronomical Journal*, *157*(2), 90. https://doi.org/10.3847/1538-3881/aafb36

Kalmoni, N. M. E., Rae, I. J., Watt, C. E. J., Murphy, K. R., Samara, M., Michell, R. G., et al. (2018). A diagnosis of the plasma waves responsible for the explosive energy release of substorm onset. *Nature Communications*, *9*(1), 4806. https://doi.org/10.1038/s41467-018-07086-0

Kimura, T., Nichols, J. D., Gray, R. L., Tao, C., Murakami, G., Yamazaki, A., et al. (2017). Transient brightening of Jupiter's aurora observed by the Hisaki satellite and Hubble Space Telescope during approach phase of the Juno spacecraft. *Geophysical Research Letters*, *44*(10), 4523–4531. https://doi.org/10.1002/2017GL072912

Kivelson, M. G.. (2015). Planetary magnetodiscs: Some unanswered questions. *Space Science Reviews*, *187*(1), 5–21. https://doi.org/10.1007/s11214-014-0046-6

Korth, H., Zhang, Y., Anderson, B. J., Sotirelis, T., & Waters, C. L. (2014). Statistical relationship between large-scale upward field-aligned currents and electron precipitation. *Journal of Geophysical Research: Space Physics*, *119*(8), 6715–6731. https://doi.org/10.1002/2014JA019961

Kronberg, E. A., Glassmeier, K.-H., Woch, J., Krupp, N., Lagg, A., & Dougherty, M. K. (2007). A possible intrinsic mechanism for the quasi-periodic dynamics of the Jovian magnetosphere. *Journal of Geophysical Research*, *112*, A05203. https://doi.org/10.1029/2006JA011994

Kronberg, E. A., Woch, J., Krupp, N., Lagg, A., Daly, P. W., & Korth, A. (2008). Comparison of periodic substorms at Jupiter and Earth: Periodic substorms at Jupiter and Earth. *Journal of Geophysical Research*, *113*, A04212. https://doi.org/10.1029/2007JA012880

Kronberg, E. A., Woch, J., Krupp, N., Lagg, A., Khurana, K. K., & Glassmeier, K.-H. (2005). Mass release at Jupiter: Substorm-like processes in the Jovian magnetotail. *Journal of Geophysical Research*, *110*, A03211. https://doi.org/10.1029/2004JA010777

Krupp, N., Woch, J., Lagg, A., Wilken, B., Livi, S., & Williams, D. J. (1998). Energetic particle bursts in the predawn Jovian magnetotail. *Geophysical Research Letters*, *25*(8), 1249–1252. https://doi.org/10.1029/98GL00863

Kullen, A., & Karlsson, T. (2004). On the relation between solar wind, pseudobreakups, and substorms. *Journal of Geophysical Research*, *109*, A12218. https://doi.org/10.1029/2004JA010488

Liou, K., Newell, P. T., Zhang, Y.-L., & Paxton, L. J. (2013). Statistical comparison of isolated and non-isolated auroral substorms. *Journal of Geophysical Research: Space Physics*, *118*(5), 2466–2477. https://doi.org/10.1002/jgra.50218

Louarn, P., Paranicas, C. P., & Kurth, W. S. (2014). Global magnetodisk disturbances and energetic particle injections at Jupiter. *Journal of Geophysical Research: Space Physics*, *119*(6), 4495–4511. https://doi.org/10.1002/2014JA019846

Louarn, P., Roux, A., Perraut, S., Kurth, W. S., & Gurnett, D. A. (2000). A study of the Jovian "energetic magnetospheric events" observed by Galileo: Role in the radial plasma transport. *Journal of Geophysical Research*, *105*(A6), 13073–13088. https://doi.org/10.1029/1999JA900478

Lui, A. T. Y. (2015). Magnetospheric Substorm onset by current disruption processes. In Y. Zhang, & L. J. Paxton (Eds.), *Auroral dynamics and space weather* (pp. 163–176). American Geophysical Union (AGU). https://doi.org/10.1002/9781118978719.ch12

Lui, A. T. Y., Chang, C.-L., Mankofsky, A., Wong, H.-K., & Winske, D. (1991). A cross-field current instability for substorm expansions. *Journal of Geophysical Research*, *96*(A7), 11389–11401. https://doi.org/10.1029/91JA00892

Manners, H., Masters, A., & Yates, J. N. (2018). Standing Alfvén waves in Jupiter's magnetosphere as a source of ~10- to 60-Min quasiperiodic pulsations. *Geophysical Research Letters*, *45*(17), 8746–8754. https://doi.org/10.1029/2018GL078891

Masters, A. (2017). Model-based assessments of magnetic reconnection and Kelvin-Helmholtz instability at Jupiter's magnetopause. *Journal of Geophysical Research: Space Physics*, *122*, 11154–11174. https://doi.org/10.1002/2017JA024736

Mauk, B., & Bagenal, F. (2013). Comparative auroral physics: Earth and other planets. In A. Keiling, E. Donovan, F. Bagenal, & T. Karlsson (Eds.), *Auroral phenomenology and magnetospheric processes: Earth and other planets* (pp. 3–26). American Geophysical Union (AGU). https://doi.org/10.1029/2011GM001192

Mauk, B. H., Williams, D. J., & McEntire, R. W. (1997). Energy-time dispersed charged particle signatures of dynamic injections in Jupiter's inner magnetosphere. *Geophysical Research Letters*, *24*(23), 2949–2952. https://doi.org/10.1029/97GL03026

Miyashita, Y., & Ieda, A. (2018). Revisiting substorm events with preonset aurora. *Annales Geophysicae*, *36*(5), 1419–1438. https://doi.org/10.5194/angeo-36-1419-2018

Mura, A., Adriani, A., Altieri, F., Connerney, J. E. P., Bolton, S. J., Moriconi, M. L., et al. (2017). Infrared observations of Jovian aurora from Juno's first orbits: Main oval and satellite footprints. *Geophysical Research Letters*, *44*, 5308–5316. https://doi.org/10.1002/2017GL072954

Murphy, K. R., Mann, I. R., Rae, I. J., Walsh, A. P., & Frey, H. U. (2014). Inner magnetospheric onset preceding reconnection and tail dynamics during substorms: Can substorms initiate in two different regions? *Journal of Geophysical Research: Space Physics*, *119*(12), 9684–9701. https://doi.org/10.1002/2014JA019795

Nichols, J. D., Clarke, J. T., Gérard, J. C., Grodent, D., & Hansen, K. C. (2009). Variation of different components of Jupiter's auroral emission. *Journal of Geophysical Research*, *114*(A13), A06210. https://doi.org/10.1029/2009JA014051

Nishimura, Y., Lyons, L. R., Angelopoulos, V., Kikuchi, T., Zou, S., & Mende, S. B. (2011). Relations between multiple auroral streamers, pre-onset thin arc formation, and substorm auroral onset. *Journal of Geophysical Research*, *116*, A09214. https://doi.org/10.1029/2011JA016768

Nishimura, Y., Lyons, L., Zou, S., Angelopoulos, V., & Mende, S. (2010). Substorm triggering by new plasma intrusion: THEMIS all-sky imager observations. *Journal of Geophysical Research*, *115*, A07222. https://doi.org/10.1029/2009JA015166

Oberhagemann, L. R., & Mann, I. R. (2020). A new substorm onset mechanism: Increasingly parallel pressure anisotropic ballooning. *Geophysical Research Letters*, *47*(2), e2019GL085271. https://doi.org/10.1029/2019GL085271

Panov, E. V., Lu, S., & Pritchett, P. L. (2020). Understanding spacecraft trajectories through detached magnetotail interchange heads. *Journal of Geophysical Research: Space Physics*, *125*(5), e2020JA027930. https://doi.org/10.1029/2020JA027930

Pulkkinen, T. I., Baker, D. N., Wiltberger, M., Goodrich, C., Lopez, R. E., & Lyon, J. G. (1998). Pseudobreakup and substorm onset: Observations and MHD simulations compared. *Journal of Geophysical Research*, *103*(A7), 14847–14854. https://doi.org/10.1029/97JA03244

Radioti, A., Grodent, D., Gérard, J.-C., Bonfond, B., Gustin, J., Pryor, W., et al. (2013). Auroral signatures of multiple magnetopause reconnection at Saturn. *Geophysical Research Letters*, *40*(17), 4498–4502. https://doi.org/10.1002/grl.50889

Radioti, A., Grodent, D., Gérard, J.-C., Vogt, M. F., Lystrup, M., & Bonfond, B. (2011). Nightside reconnection at Jupiter: Auroral and magnetic field observations from 26 July 1998. *Journal of Geophysical Research*, *116*, A03221. https://doi.org/10.1029/2010JA016200

Radioti, A., Yao, Z., Grodent, D., Palmaerts, B., Roussos, E., Dialynas, K., et al. (2019). Auroral beads at Saturn and the driving mechanism: Cassini proximal orbits. *The Astrophysical Journal*, *885*(1), L16. https://doi.org/10.3847/2041-8213/ab4e20

Rostoker, G., Akasofu, S.-I., Foster, J., Greenwald, R. A., Kamide, Y., Kawasaki, K., et al. (1980). Magnetospheric substorms – Definition and signatures. *Journal of Geophysical Research*, *85*(A4), 1663–1668. https://doi.org/10.1029/JA085iA04p01663

Sergeev, V. A., Kornilova, T. A., Kornilov, I. A., Angelopoulos, V., Kubyshkina, M. V., Fillingim, M., et al. (2010). Auroral signatures of the plasma injection and dipolarization in the inner magnetosphere. *Journal of Geophysical Research*, *115*, A02202. https://doi.org/10.1029/2009JA014522

Swithenbank-Harris, B., Nichols, J., Allegrini, F., Bagenal, F., Bonfond, B., Bunce, E., et al. (2021). Simultaneous Observation of an Auroral Dawn Storm with the Hubble Space Telescope and Juno. *Journal of Geophysical Research: Space Physics*.

Tao, C., Kataoka, R., Fukunishi, H., Takahashi, Y., & Yokoyama, T. (2005). Magnetic field variations in the Jovian magnetotail induced by solar wind dynamic pressure enhancements. *Journal of Geophysical Research*, *110*, A11208. https://doi.org/10.1029/2004JA010959

Vasyliunas, V. M. (1983). Physics of the Jovian magnetosphere. In A. J. Dessler (Ed.), *Physics of the Jovian magnetosphere* (pp. 395–453). Cambridge University Press.

Viñas, A. F., & Madden, T. R. (1986). Shear flow-ballooning instability as a possible mechanism for hydromagnetic fluctuations. *Journal of Geophysical Research*, *91*(A2), 1519–1528. https://doi.org/10.1029/JA091iA02p01519

Vogt, M. F., Bunce, E. J., Kivelson, M. G., Khurana, K. K., Walker, R. J., Radioti, A., et al. (2015). Magnetosphere-ionosphere mapping at Jupiter: Quantifying the effects of using different internal field models. *Journal of Geophysical Research: Space Physics*, *120*(4), 2584–2599. https://doi.org/10.1002/2014JA020729

Vogt, M. F., Gyalay, S., Kronberg, E. A., Bunce, E. J., Kurth, W. S., Zieger, B., & Tao, C. (2019). Solar wind interaction with Jupiter's magnetosphere: A statistical study of galileo in situ data and modeled upstream solar wind conditions. *Journal of Geophysical Research: Space Physics*, *124*(12), 10170–10199. https://doi.org/10.1029/2019JA026950

Vogt, M. F., Kivelson, M. G., Khurana, K. K., Joy, S. P., & Walker, R. J. (2010). Reconnection and flows in the Jovian magnetotail as inferred from magnetometer observations. *Journal of Geophysical Research*, *115*, A06219. https://doi.org/10.1029/2009JA015098

Woch, J., Krupp, N., & Lagg, A. (2002). Particle bursts in the Jovian magnetosphere: Evidence for a near-Jupiter neutral line. *Geophysical Research Letters*, *29*(7), 42-1–42-4. https://doi.org/10.1029/2001GL014080

Yao, Z. H., Bonfond, B., Clark, G., Grodent, D., Dunn, W. R., Vogt, M. F., et al. (2020a). Reconnection- and dipolarization-driven auroral dawn storms and injections. *Journal of Geophysical Research: Space Physics*, *125*, e2019JA027663. https://doi.org/10.1029/2019JA027663

Yao, Z. H., Bonfond, B., Grodent, D., Chané, E., Dunn, W. R., Kurth, W. S., et al. (2020b). *Auroral diagnosis of solar wind interaction with Jupiter's magnetosphere*. Retrieved from http://arxiv.org/abs/2004.10140

Yao, Z., Pu, Z. Y., Rae, I. J., Radioti, A., & Kubyshkina, M. V. (2017). Auroral streamer and its role in driving wave-like pre-onset aurora. *Geoscience Letters*, *4*(1), 8. https://doi.org/10.1186/s40562-017-0075-6

Zhang, B., Delamere, P. A., Yao, Z., Bonfond, B., Lin, D., Sorathia, K. A., et al. (2020). *How Jupiter's unusual magnetospheric topology structures its aurora*. ArXiv E-Prints 2006, arXiv:2006.14834